Anomalous Coherent Backscattering of Light from Opal Photonic Crystals

J. Huang, N. Eradat, M. E. Raikh, and Z. V. Vardeny
Department of Physics, University of Utah, Salt Lake City, Utah 84112

A. A. Zakhidov and R. H. Baughman
Honeywell International, Research and Technology Center, Morristown, New Jersey 07962
(Received 28 November 2000)

We studied coherent backscattering (CBS) of light from opal photonic crystals with incomplete band gaps. We observed a dramatic broadening of the CBS cone for incident angles close to the Bragg condition in the crystals. We modify the conventional CBS theory to incorporate Bragg attenuation resulting from the photonic band structure. By fitting the CBS data with the modified theory, we extract *both* the *disorder-induced* light mean-free path and the Bragg attenuation length of the *inherent* opal photonic crystal.

DOI: 10.1103/PhysRevLett.86.4815 PACS numbers: 42.70.Qs, 42.25.Dd, 71.55.Jv

The underlying physics of coherent backscattering (CBS) of light from a disordered medium is a constructive interference of waves traversing the same sequence of scatterers in clockwise and anticlockwise directions. This interference results in the enhancement of the reflected intensity (albedo) within a narrow cone with angular width $\Delta\theta \sim \lambda_L/l^*$ around the angle of incidence. Here, λ_L and l^* are the laser light wavelength and mean-free path, respectively. Following the pioneering experiments on microsphere suspensions [1], the observation of the CBS cone was later reported for a variety of random media ranging from regolithic ice grains covering the particles of Saturn's rings [2] to laser-cooled gas of rubidium atoms [3].

Universality of the mechanism leading to the CBS cone formation manifests itself in the fact that the shapes of the cones in the albedo, $\alpha(\delta\theta)$, where $\delta\theta$ is the angular deviation from the backscattering direction, are remarkably similar in the various experiments. On the quantitative side, the width of the CBS cone yields the value of the light mean-free path, l^*. In fact, despite the conceptual elegance of the CBS effect, the value of l^* is the only quantitative information it has provided so far. We note, however, that l^* in disordered media can be also determined from more conventional measurements of the transmission versus thickness [4] which do not rely on the interference of reciprocal scattering paths.

In this Letter, we report on CBS measurements performed in optically *periodic* structures *with disorder,* specifically synthetic opal photonic crystals. Our main finding is that even a weak periodicity significantly affects the backscattering albedo for certain angles of incidence, θ, close to the Bragg condition in the sample [5]. By measuring the evolution of the CBS cone with θ, we were able to extract from the data both the value of l^*, which is the characteristic of the disorder, and width of the incomplete photonic band gap of the *inherent* periodic structure along $\langle 111 \rangle$. The ability to separate the two effects of disorder and periodicity reveals the unique potential of the CBS technique.

For our studies of periodic structures, we have chosen the synthetic air-filled opals, which crystallize in a fcc lattice of monodispersed silica (SiO_2) spheres with a diameter, $\mathcal{D} = 295$ nm, within 4%. Details of the opal fabrication and their mechanical properties are reported in Ref. [6]. In contrast to photonic crystals with *complete* band gaps, that have recently attracted a lot of attention because of possible optical device applications [7,8], the periodicity-induced stop bands of synthetic opals are *incomplete* gaps where light propagation is forbidden only along certain directions. Along these directions and for frequencies within the gap, the incident light intensity decays away from the boundary with a certain decrement L_B—that is the Bragg attenuation length. When disorder is negligible, then L_B and, correspondingly, the photonic gap width can be deduced from reflectivity measurements. However, in reality, disorder is present in the samples causing the Bragg reflectivity peak to broaden dramatically [9]. Under these conditions determination of L_B is a challenge.

For our CBS measurements, we cut a centimeter-size opal single crystal along the (111) surface. We used a standard experimental setup to measure the albedo with angular resolution in $\delta\theta$ of less than 1 mrad [10]. The coherent light beam was directed from several continuous wave lasers such as Ar^+ and HeNe, as well as various well-collimated semiconductor lasers. The laser beam was linearly polarized with transverse electric field (TE) polarization. The reflected intensity from the opal surface with TE polarization was measured versus $\delta\theta$ using a silicon detector and phase-sensitive techniques. The incident beam (5 mm in diameter) was directed at various angles, θ between $-30°$ to $70°$ relative to the surface normal, and $\delta\theta$ was varied within 200 mrad. To obtain speckle-free CBS cones, we performed configuration averaging using three different methods [11]. These include different illuminated areas of the opal surface, different inclination angles ($\varphi < 2°$) of the illuminated surface with respect to the laser beam, and sample rotation about the normal direction to the crystal surface.

In Fig. 1, we show typical CBS cones measured at various incident angles θ that we obtained using an Ar^+ laser at $\lambda_L = 515$ nm. The CBS cones are apparent in all cases and their width, $\Delta\theta_{1/4}$ at quarter maximum versus θ, is summarized in Fig. 2 (inset). It is seen that $\Delta\theta_{1/4}(\theta)$ exhibits a pronounced anomaly in the form of a sharp maximum within a narrow interval $\gamma \approx 5°$ around $\theta = 42°$. This maximum in $\Delta\theta_{1/4}(\theta)$ is superimposed on a monotonic $\Delta\theta_{1/4}$ increase at large θ. Within the interval γ, the width $\Delta\theta_{1/4}$ exceeds the background value by about a factor of 1.5. The CBS cones in Fig. 1 were fitted using the standard expression [12] for the coherent albedo, α_c, from a disordered medium occupying a half-space, $z > 0$,

$$\alpha_c(\theta, \delta\theta) \propto \frac{1}{(1 + k_\perp l^* \cos\phi)^2}\left[\frac{1 - e^{-2k_\perp z_0}}{k_\perp l^* \cos\phi} + 1\right], \tag{1}$$

where ϕ is the propagation angle inside the medium, which is related to θ through Snell's law; $\delta\theta$ enters into the right-hand side of Eq. (1) through $k_\perp = 2\pi \cos\theta\, \delta\theta/\lambda_L$. The meaning of $k_\perp$ is the difference between the in-plane components of the wave vectors of incoming and outgoing light *inside* the medium. In Eq. (1), $z_0 = 0.7l^*$ originates from the "trapping plane" [12] at $z = -z_0$, which is introduced to account for the fact that light propagation in the disordered medium occurs in the presence of the boundary at $z = 0$. It is convenient to rewrite the combination $k_\perp l^* \cos\phi$ in Eq. (1) as a ratio $\delta\theta/\Delta\theta$, where $\Delta\theta = \lambda_L/(2\pi l^* \cos\theta \cos\phi)$ is the effective cone width.

The above fitting procedure was repeated for all measured incident angles. $\Delta\theta(\theta)$ that parametrizes the CBS cones at various θ is shown in Fig. 2. We note that the anomaly around $\theta = 42°$ is more accentuated in $\Delta\theta(\theta)$ than in $\Delta\theta_{1/4}(\theta)$.

Insight into the origin of the observed anomaly in $\Delta\theta(\theta)$ may be obtained from Fig. 3, where the angle-dependent normalized reflectivity spectra, $R(\lambda)$, are shown. It is seen that for $\lambda_L = 515$ nm the angle $\theta = \theta_B = 42°$, at which the anomaly in the CBS cones occurs (Fig. 2), corresponds to the Bragg condition $\lambda_L = 2d\sqrt{n_{\mathrm{eff}}^2 - \sin^2\theta_B}$, where $d = (\frac{2}{3})^{1/2}\mathcal{D} \approx 243$ nm is the interplane distance along [111], and $n_{\mathrm{eff}} \approx 1.3$ is the opal effective refraction index. In order to test this observation, we studied [11] the evolution of the $\Delta\theta$ anomaly with the wavelength of the incident light beam. The angle at which the CBS anomaly occurred followed the measured dependence $\theta_B(\lambda_L)$ shown in Fig. 3 (inset). We also observed that the $\Delta\theta$ anomaly around θ_B becomes much stronger than that in Fig. 2 for $\lambda_L = 632$ nm. The dependence $\Delta\theta(\theta)$ for this wavelength is shown in Fig. 4. The Bragg condition for $\lambda_L = 632$ nm corresponds to normal incidence [Fig. 3 (inset)]. It is seen that the incident angle interval $\gamma \approx 30°$ around $\theta = 0$, where the effective cone width is enhanced, is much larger than $\gamma \approx 5°$ measured for $\lambda_L = 515$ nm (Fig. 2). Also, the enhancement factor in $\Delta\theta$ is ~ 3 for $\lambda_L = 632$ nm (Fig. 4) compared to ~ 2 for $\lambda_L = 515$ nm in Fig. 2. Both observations, namely, the anomaly in $\Delta\theta(\theta)$ at $\theta = \theta_B$

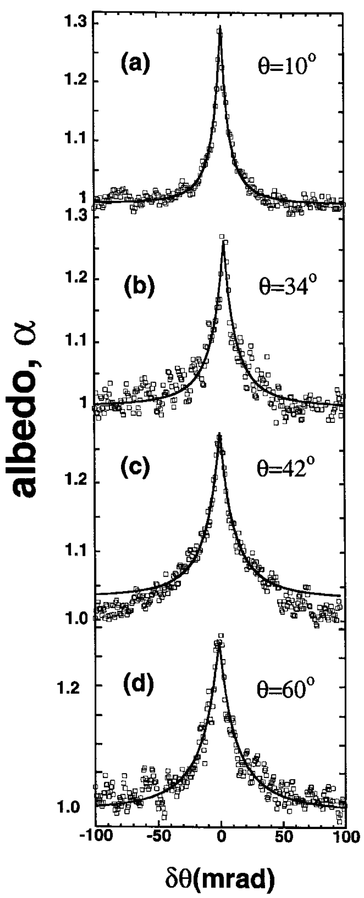

FIG. 1. Coherent backscattering cones in the albedo, α, at various incident angles, θ, measured at $\lambda_L = 515$ nm: (a) $\theta = 10°$; (b) $\theta = 34°$; (c) $\theta = 42°$; (d) $\theta = 60°$. Also shown are fits to the experimental data using Eq. (1).

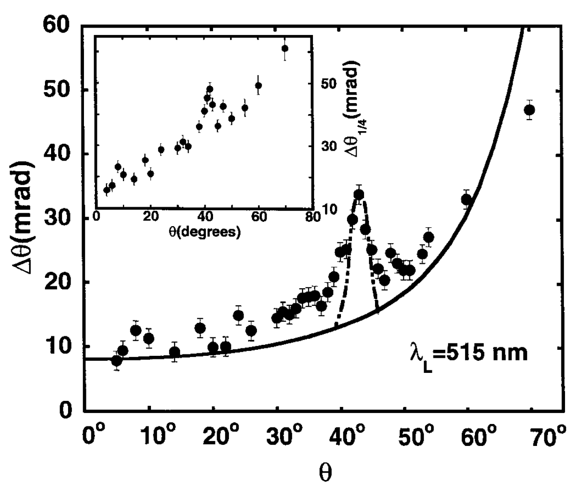

FIG. 2. The effective width, $\Delta\theta$, parametrizing the measured CBS cones extracted using Eq. (1) at $\lambda_L = 515$ nm plotted versus the incident angle, θ; the inset shows the CBS cone width at quarter maximum, $\Delta\theta_{1/4}$ versus θ. The solid line is $\Delta\theta$ calculated using Eq. (1) with a single parameter $l^* = 7.2\ \mu$m; the dashed-broken line around $\theta_B = 42°$ that describes the Bragg-related CBS anomaly is calculated using Eq. (3) with $l^* = 7.2\ \mu$m and $L_B = 5.1\ \mu$m.

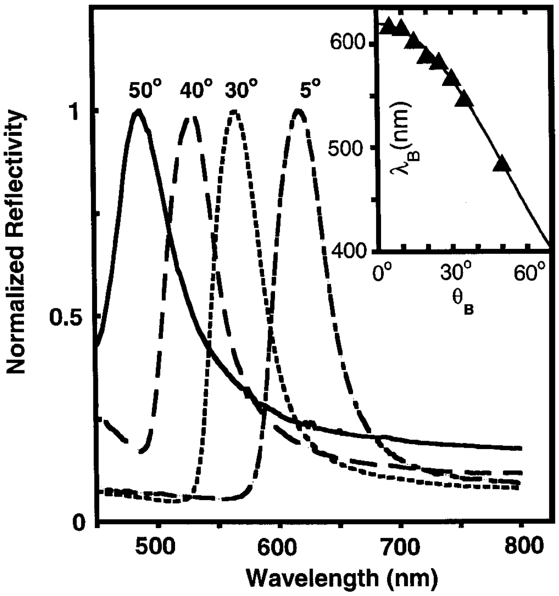

FIG. 3. Normalized reflectivity spectra for various Bragg angles. The inset shows the wavelength of the Bragg band, $\lambda_B(\theta_B)$. The solid line is a fit using the relation, $\lambda_B(\theta_B) = 2d\sqrt{n_{\rm eff}^2 - \sin^2\theta_B}$, with $d = 243$ nm and $n_{\rm eff} = 1.3$.

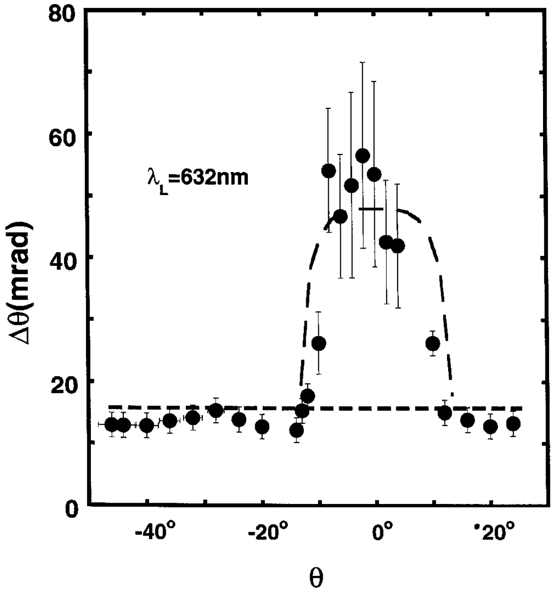

FIG. 4. The effective width, $\Delta\theta$, of CBS cones measured at various θ around $\theta = 0$ using $\lambda_L = 632$ nm, for which $\theta_B \approx 0$. The dashed line is calculated using Eq. (4).

and a dramatic strengthening of the anomaly at $\theta_B \approx 0$, require an explanation.

We start by examining a *general* expression for the coherent scattering albedo from a disordered medium [12], which, in the case of a *homogeneous* medium, leads to Eq. (1). The albedo, $\alpha(\theta, \theta')$, at an angle θ' due to an incident light beam at an angle θ is determined by the first and last light scattering events occurring at the spatial points $\mathbf{r}$ and $\mathbf{r}'$, respectively, and by the light diffusion process that occurs between these events. If z and z' are the projections of $\mathbf{r}$ and $\mathbf{r}'$ on the z axis, and ρ is the projection of $(\mathbf{r} - \mathbf{r}')$ on the plane $z = 0$, then the coherent part, α_c, of the albedo, α, is given by the expression

$$\begin{aligned}\alpha_c(\theta, \theta') \propto \int_0^\infty dz\, dz' \int d^2\rho\, \mathcal{P}_\phi(z) \\ \times \{\cos[k_\perp \rho + k(\cos\phi - \cos\phi')(z - z')]\} \\ \times \Pi(\rho, z, z')\mathcal{P}_{\phi'}(z') . \qquad (2)\end{aligned}$$

Here $k = 2\pi n_{\rm eff}/\lambda_L$. Analogously to ϕ and θ, the angles ϕ' and θ' are related through Snell's law. In Eq. (2), $\mathcal{P}_\phi(z)$ is the probability density for the incident light to propagate up to the depth z *before* the occurrence of the *first* scattering event. Analogously, $\mathcal{P}_{\phi'}(z')$ is the surviving probability density *after* the occurrence of the *last* scattering event. $\mathcal{P}_{\phi'}(z')$ has the same form as $\mathcal{P}_\phi(z)$, where ϕ, z are replaced by ϕ', z', respectively. The propagator $\Pi(\rho, z, z')$ in Eq. (2) describes the diffusive motion of light between the first and the last scattering events.

Expression (2) is quite general, and it also applies in the presence of a periodic modulation of the refraction index in the z direction, if this modulation is properly incorporated into the probabilities $\mathcal{P}(z)$ and the propagator $\Pi(\rho, z, z')$. Our key observation is that for a weak modulation and, consequently, for a relatively narrow incomplete gap in the photonic band structure, the propagator is affected very little by Bragg diffraction. Indeed, the angle interval around θ_B in which the diffraction is strong can be estimated as $\delta\theta_B \sim d/L_B \sim \delta\lambda_L/\lambda_L \ll 1$, where $\delta\lambda_L$ is the gap spectral width. On the other hand, in the course of the *diffusion* process, light explores *all* propagation directions within the solid angle 4π. As an upper estimate for $\delta\lambda_L$ in our experiment, we may take the width of the reflectivity spectra in Fig. 3, although they are broadened by disorder. Even under these conditions, we get $\delta\lambda_L/\lambda_L \approx 0.09$. This allows us to use for the propagator $\Pi(\rho, z, z')$ the conventional expression [12], which is valid for a semi-infinite *homogeneous* medium, namely, $\Pi(\rho, z, z') = \Pi_0(\rho, z, z') - \Pi_0(\rho, z, z'^*)$, where $\Pi_0(\rho, z, z') = (4\pi D\sqrt{(z - z')^2 + \rho^2})^{-1}$ is the diffusion propagator in an unbounded medium; $D = l^*c/3$ is the light diffusion coefficient, and z'^* is the mirror image of z' with respect to the trapping plane $z = -z_0$. The choice of the above propagator ensures that the boundary conditions $\Pi(\rho, -z_0, z') = \Pi(\rho, z, -z_0) = 0$ are obeyed.

We now turn to the probability density $\mathcal{P}_\phi(z)$. For incident angle θ away from θ_B, we have [12] $\mathcal{P}_\phi(z) = (l^* \cos\phi)^{-1} \exp(-z/l^* \cos\phi)$. For $\theta \approx \theta_B$, the light intensity decays as $\exp(-z/L_B)$ due to the Bragg attenuation. The factor $\exp(-z/L_B)$ can be interpreted as the probability to *survive* the Bragg diffraction. Therefore, at $\theta = \theta_B$, $\mathcal{P}_\phi(z)$ represents the *joint* surviving probability, and thus can be written as a single exponent $\exp(-z/l^*_{\rm eff} \cos\phi_B)$, where $(l^*_{\rm eff})^{-1} = (l^*)^{-1} + \cos\phi_B L_B^{-1}$. Naturally, $\mathcal{P}_{\phi'}(z')$ should be modified in a similar way.

If both θ and θ' are close, but not equal to θ_B, then Bragg attenuation becomes weaker. It can be shown that this effect is taken into account by the following modification of $l^*_{\rm eff}(\phi)$:

$$\frac{1}{l^*_{\rm eff}(\phi)} = \frac{1}{l^*} + \frac{\cos\phi_B}{L_B}\sqrt{1 - \left(\frac{\theta - \theta_B}{\gamma_1}\right)^2}, \tag{3}$$

where $\gamma_1 = \lambda_L\sqrt{n^2_{\rm eff} - \sin^2\theta_B}/\pi L_B \sin(2\theta_B)$ is the angular width of the Bragg gap. The above expression was derived under the assumption $|\theta - \theta_B| \ll \theta_B$. For small $\theta_B \lesssim (d/L_B)^{1/2}$, this assumption is no longer valid and Eq. (3) should be replaced by

$$\frac{1}{l^*_{\rm eff}(\phi)} = \frac{1}{l^*} + \frac{1}{L_B}\sqrt{1 - \left(\frac{\theta}{\gamma_2}\right)^4}, \tag{4}$$

where $\gamma_2 = \sqrt{\lambda_L n_{\rm eff}/\pi L_B}$. We thus conclude that the effect of periodic modulation amounts to the replacement $l^* \to l^*_{\rm eff}$ in the surviving probabilities $\mathcal{P}_\phi(z)$ and $\mathcal{P}_{\phi'}(z')$. Therefore, the evaluation of the integrals in Eq. (2) reproduces Eq. (1) for the coherent albedo with $l^*_{\rm eff}$ instead of l^*. Note, however, that z_0 in Eq. (1), which originates from the propagator Π, is determined by the "bare" l^* value, namely, $z_0 = 0.7l^*$.

Equation (1) together with Eqs. (3) and (4) allow us to account for the obtained CBS anomalies in Figs. 2 and 4. First, we focus on the domain of θ outside the Bragg gap where $l^*_{\rm eff} = l^*$, so that Eq. (1) contains only a single free parameter, l^*. We determined l^* by fitting the data for $\Delta\theta(\theta)$ in Fig. 2, and obtained $l^* = 7.2\ \mu$m. The theoretical dependence $\Delta\theta(\theta)$ calculated with this value of l^* for $\lambda_L = 515$ nm is shown in Fig. 2 (solid line). It is seen that a *single* l^* provides a good agreement with the experimental data within the entire interval $\theta < 70°$, except for $\theta \approx \theta_B$. Once l^* was determined, we were able to extract the value of L_B by fitting $\Delta\theta(\theta)$ around $\theta = \theta_B$ (Fig. 2) using Eq. (1) with $l^*_{\rm eff}$ given by Eq. (3). This fit yields $L_B = 5.1\ \mu$m; the overall good agreement of the modified theory with the data for $\Delta\theta(\theta)$ in the vicinity of $\theta_B = 42°$ shown in Fig. 2 is apparent.

According to Eq. (3), $l^*_{\rm eff}$ is smaller than l^* thus causing broadening of the CBS cone for θ within the interval $|\theta - \theta_B| < \gamma_1$. With the obtained $L_B = 5.1\ \mu$m, we calculated the angular width of the CBS anomaly to be $2\gamma_1 = 4°$ at $\lambda_L = 515$ nm in agreement with the measurements (Fig. 2). We also calculated the spectral width of the inherent Bragg gap to be $\delta\lambda_L/\lambda_L \approx 0.03$. We note that this value is 3 times smaller than $\delta\lambda_L/\lambda_L \approx 0.09$ extracted from $R(\lambda)$ spectra in Fig. 3. This illustrates the ambiguity in determining the photonic band structure from reflectivity measurements.

When the Bragg angle is small, then the width of the CBS anomaly is equal to $2\gamma_2$, as follows from Eq. (4). Using $L_B = 5.1\ \mu$m, we found for $\lambda_L = 632$ nm $2\gamma_2 = 26°$, which is much larger than $2\gamma_1$ and agrees well with the data in Fig. 4. Moreover, from Eq. (4) we calculated the theoretical curve $\Delta\theta(\theta)$ shown in Fig. 4. This curve reproduces very well the enhancement of the effective cone width at $\theta_B = 0$.

In conclusion, we demonstrated that the remarkable universality of the CBS characteristics for diverse disordered materials does not hold for photonic crystals at near Bragg conditions. We have shown that the Bragg attenuation length and, consequently, the photonic band gap of the inherent crystal, as well as the light mean-free path, can be readily extracted from the CBS measurements even if they are comparable in magnitude. For $L_B \lesssim l^*$, disorder is unable to completely mask the contribution of Bragg diffraction to the CBS inside the photonic crystal. The reason for that is that CBS involves *free* light propagation *before the first* and *after the last* scattering events, when the existing disorder is *not yet relevant.* This makes the CBS measurements a much more sensitive tool for characterizing the inherent band structure of disordered photonic crystals as compared to the more conventional measurements of optical reflectivity.

This work was supported by NSF under Grant No. DMR 9732820, by the Army Research Office under Grant No. DAAD 19-0010406, and the Petroleum Research Fund under Grant ACS-PRF No. 34302-AC6.

[1] Y. Kuga and A. Ishimaru, J. Opt. Soc. Am. A **1**, 831 (1984); M. P. van Albada and A. Lagendijk, Phys. Rev. Lett. **55**, 2692 (1985); P. E. Wolf and G. Maret, Phys. Rev. Lett. **55**, 2696 (1985).

[2] M. I. Mishchenko, Astrophys. J. **411**, 351 (1993).

[3] G. Labeyrie *et al.,* Phys. Rev. Lett. **83**, 5266 (1999).

[4] A. Z. Genack, Phys. Rev. Lett. **58**, 2043 (1987).

[5] Similar experiments recently performed on TiO_2-based photonic crystals [A. F. Koenderink *et al.,* Phys. Lett. A **268**, 104 (2000)] by changing the impinging wavelength did not reveal this effect.

[6] A. A. Zakhidov *et al.,* Science **282**, 897 (1998).

[7] E. Yablonovitch, Phys. Rev. Lett. **58**, 2059 (1987); S. John, *ibid.* **58**, 2486 (1987).

[8] *Photonic Band Gaps and Localization,* edited by C. M. Soukoulis (Plenum, New York, 1993); J. D. Joannopoulos, R. D. Meade, and J. N. Winn, *Photonic Crystals: Molding the Flow of Light* (Princeton University Press, Princeton, New Jersey, 1995).

[9] It has recently been demonstrated [Yu. A. Vlasov, M. Deutch, and D. J. Norris, Appl. Phys. Lett. **76**, 1627 (2000)] that the contribution to broadening of the reflectivity spectra caused by domain boundaries in opal photonic crystals can be eliminated by spatially resolved measurements.

[10] S. Etemad, R. Thompson, and M. J. Andrejco, Phys. Rev. Lett. **57**, 575 (1986); M. Kaveh *et al., ibid.* **57**, 2049 (1986).

[11] J. Huang, Ph.D. thesis, University of Utah, 2000 (unpublished).

[12] E. Akkermans, P. E. Wolf, and R. Maynard, Phys. Rev. Lett. **56**, 1471 (1986); E. Akkermans *et al.,* J. Phys. (Paris) **49**, 77 (1988).